The Journal of Chemical Physics

Surface hopping with a manifold of electronic states. III. Transients, broadening, and the Marcus picture

Cite as: J. Chem. Phys. **142**, 234106 (2015); https://doi.org/10.1063/1.4922513
Submitted: 04 April 2015 • Accepted: 03 June 2015 • Published Online: 17 June 2015

Wenjie Dou, Abraham Nitzan and Joseph E. Subotnik

Surface hopping with a manifold of electronic states. III. Transients, broadening, and the Marcus picture

Wenjie Dou,[1] Abraham Nitzan,[2] and Joseph E. Subotnik[1]
[1]*Department of Chemistry, University of Pennsylvania, Philadelphia, Pennsylvania 19104, USA*
[2]*School of Chemistry, The Sackler Faculty of Science, Tel Aviv University, Tel Aviv 69978, Israel*

(Received 4 April 2015; accepted 3 June 2015; published online 17 June 2015)

In a previous paper [Dou *et al.*, J. Chem. Phys. **142**, 084110 (2015)], we have introduced a surface hopping (SH) approach to deal with the Anderson-Holstein model. Here, we address some interesting aspects that have not been discussed previously, including transient phenomena and extensions to arbitrary impurity-bath couplings. In particular, in this paper we show that the SH approach captures phonon coherence beyond the secular approximation, and that SH rates agree with Marcus theory at steady state. Finally, we show that, in cases where the electronic tunneling rate depends on nuclear position, a straightforward use of Marcus theory rates yields a useful starting point for capturing level broadening. For a simple such model, we find I-V curves that exhibit negative differential resistance. © *2015 AIP Publishing LLC.* [http://dx.doi.org/10.1063/1.4922513]

I. INTRODUCTION

Electron transfer between a molecule and a metal electrode is a fundamental reaction that underlies all electrochemical and molecular electronic processes as well as many phenomena involved in corrosion and heterogeneous catalysis. The Anderson-Holstein (AH) model (see Eqs. (1)–(4)) is a simple model to describe such a system, where an electronic impurity level couples both to an electronic bath and to nuclear motion.[1] For simplicity, in this paper we will not consider electron-electron (el-el) repulsion which is a source of rich physics that must be treated carefully.[2] Even without el-el repulsion, the AH model has so many degrees of freedom (DOF) that it admits no simple solution. Numerical Renormalization Group (NRG),[3–5] Multi-Configuration Time-Dependent Hartree (MCTDH),[6] and Path Integral Monte Carlo (PIMC)[7] can produce numerical exact solutions, but likely none of these methods is feasible if we seek to extend the AH model to more complicated, realistic Hamiltonians. If we are interested in approximate solutions, which do not treat the bath explicitly, Influence Functionals (IF)[8] and Nonequilibrium Green functions (NEGF)[9–13] offer alternative tools whereby one focuses on a subsystem with a handful of DOF.

Besides the methods above, historically surface hopping (SH)[14,15] has been a widely used tool for treating electron-phonon (e-ph) couplings for molecules or atoms if there are only a few electronic DOF. In the presence of a manifold of electronic DOF—for instance, the case of a loosely bound anion—Preston's surface leaking algorithm[16,17] is one possible approach. More generally, near a metal surface, Shenvi *et al.* have suggested discretizing the electronic bath, and running SH on a large number of independent potential energy surfaces (PESs).[18–20] A nonequilibrium version of the Shenvi algorithm might be possible in the vein of Refs. 21–26.

In a previous paper,[27] which we refer to as Paper II, we have analyzed an alternative approach based on a classical master equation (CME) that describes the dynamics of the AH impurity subsystem. This CME is solved by a SH approach—basically one runs trajectories on two diabatic PESs with stochastic hops between them. By further implementing level broadening, we have shown that equilibrium and out of equilibrium observables agree well with the results from NRG and the secular quantum master equation (sQME) in a classical regime (i.e., high temperature).

In the present paper, we address some interesting aspects of the CME/SH approach that were not discussed in Paper II. First, we will look at transient dynamics of the impurity electronic population. Second, we will show how our SH approach recovers the Marcus rate analytically. Third, we will generalize the AH model to the case where the impurity hybridization function depends on the nuclear coordinate, which is very relevant for processes dominated by the dynamics of the impurity-surface distance such as chemisorption[28] and surface scattering.[18,29] Fourth, in the latter case, we will investigate how to implement level broadening and show that the Marcus rate is an appealing approximation for this broadening. Fifth and finally, we will study a set of out of equilibrium I-V curves, and we will demonstrate interesting turnover effects that involve inelastic electron transport properties.[10,30]

We organize the paper as follows. In Sec. II, we outline how to derive the CME and discuss the transient observables. In Sec. III, we show that SH recovers a Marcus rate, and then we use that Marcus rate to include level broadening. We compare our results with NRG results for electron population in Sec. IV. In Sec. V, we show how one can find I-V curves that exhibit negative differential resistance according to SH and the quantum master equation (QME). We conclude in Sec. VI.

II. TRANSIENT DYNAMICS

A. Classical master equation

We begin our study with the AH model Hamiltonian,

$$H = H_s + H_b + H_c, \tag{1}$$

$$H_s = E_d d^+ d + g(a^+ + a)d^+ d + \hbar\omega(a^+ a + \tfrac{1}{2}), \tag{2}$$

$$H_b = \sum\nolimits_k (\epsilon_k - \mu) c_k^+ c_k, \tag{3}$$

$$H_c = \sum\nolimits_k V_k (c_k^+ d + d^+ c_k). \tag{4}$$

H_s is the system Hamiltonian, consisting of an impurity level with energy E_d coupled to an oscillator with frequency ω. The bath Hamiltonian, H_b, describes an electrode which is assumed to be in equilibrium characterized by the temperature T and the electronic chemical potential μ. H_c is the coupling between the impurity and the electrode.

The key quantity of interest is the reduced density matrix of the system. Starting with the quantum Liouville equation in the interaction picture, we find the total density matrix evolves as[31]

$$\frac{d\rho(t)}{dt} = -\frac{i}{\hbar}[H_c(t), \rho(0)] - \frac{1}{\hbar^2}\int_0^t dt'[H_c(t), [H_c(t'), \rho(t')]], \tag{5}$$

where

$$H_c(t) = \exp(i(H_s + H_b)t/\hbar) H_c \exp(-i(H_s + H_b)t/\hbar). \tag{6}$$

In the Born-Markovian approximation, we replace $\rho(t')$ by $\rho_b^{eq} \bigotimes \rho_s(t)$ in the integrand that relies on the assumptions that the bath remains in equilibrium throughout the process and that bath correlation functions decay fast on the system time scale. This leads to (setting $\tau = t - t'$)

$$\frac{d\rho(t)}{dt} = -\frac{i}{\hbar}[H_c(t), \rho(0)] - \frac{1}{\hbar^2}\int_0^\infty d\tau [H_c(t), [H_c(t-\tau), \rho_b^{eq} \bigotimes \rho_s(t)]]. \tag{7}$$

Next, we assume the initial total density matrix is a direct product of the system density matrix and the equilibrium bath density matrix, i.e., $\rho(0) = \rho_b^{eq} \bigotimes \rho_s(0)$ and take the trace of Eq. (7) over the bath degrees of freedom. This yields

$$\frac{d\rho_s(t)}{dt} = -\frac{1}{\hbar^2}\int_0^\infty d\tau Tr_b [H_c(t), [H_c(t-\tau), \rho_b^{eq} \bigotimes \rho_s(t)]]. \tag{8}$$

In Eq. (8), we have used $Tr_b(H_c(t)\rho_b^{eq}) = 0$. We can further write H_s as

$$H_s = H_0|0\rangle\langle 0| + H_1|1\rangle\langle 1|, \tag{9}$$

where $|0\rangle$ ($|1\rangle$) denotes the unoccupied (occupied) state of the impurity electron,

$$H_0 = \frac{1}{2}\hbar\omega(x^2 + p^2), \tag{10}$$

$$H_1 = E_d + \sqrt{2}gx + \frac{1}{2}\hbar\omega(x^2 + p^2), \tag{11}$$

with $x = \frac{1}{\sqrt{2}}(a^+ + a)$ and $p = \frac{i}{\sqrt{2}}(a^+ - a)$.

In what follows, we will consider processes in which the impurity initial state is either state 0 or state 1, that is,

$$\rho_s(t = 0) = \rho_0|0\rangle\langle 0| + \rho_1|1\rangle\langle 1|, \tag{12}$$

which ensures that there will be no coherence between occupied and unoccupied states at later time (with this Hamiltonian). Thus, we can write

$$\rho_s(t) = \rho_0|0\rangle\langle 0| + \rho_1|1\rangle\langle 1|. \tag{13}$$

After plugging Eq. (13) into Eq. (8), one can show that, in the Schrödinger picture, the reduced density matrix for state 0 and state 1 evolves as[31]

$$\frac{d\rho_0}{dt} = -\frac{i}{\hbar}[H_0, \rho_0] - \sum_k \frac{|V_k|^2}{\hbar^2} \times \left[\int_0^\infty d\tau e^{i\epsilon_k\tau/\hbar} f(\epsilon_k) e^{-iH_1\tau/\hbar} e^{iH_0\tau/\hbar}\rho_0 - e^{i\epsilon_k\tau/\hbar}(1 - f(\epsilon_k))\rho_1 e^{-iH_1\tau/\hbar} e^{iH_0\tau/\hbar} + h.c\right], \tag{14}$$

$$\frac{d\rho_1}{dt} = -\frac{i}{\hbar}[H_1, \rho_1] - \sum_k \frac{|V_k|^2}{\hbar^2} \times \left[\int_0^\infty d\tau e^{-i\epsilon_k\tau/\hbar}(1 - f(\epsilon_k)) e^{-iH_0\tau/\hbar} e^{iH_1\tau/\hbar}\rho_1 - e^{-i\epsilon_k\tau/\hbar} f(\epsilon_k)\rho_0 e^{-iH_0\tau/\hbar} e^{iH_1\tau/\hbar} + h.c\right]. \tag{15}$$

Here $h.c$ denotes Hermitian conjugate. Equations (14) and (15) constitute a QME. The CME is obtained by taking the Wigner transform of Eqs. (14) and (15), and throwing out all terms that are linear or higher in $\hbar$. This corresponds to a classical approximation for the nuclear motion (note that we are using dimensionless x and p here),[31]

$$\frac{\partial P_0(x,p)}{\partial t} = \frac{1}{\hbar}\frac{\partial H_0(x,p)}{\partial x}\frac{\partial P_0(x,p)}{\partial p} - \frac{1}{\hbar}\frac{\partial H_0(x,p)}{\partial p}\frac{\partial P_0(x,p)}{\partial x} - \gamma_{0\to 1}P_0(x,p) + \gamma_{1\to 0}P_1(x,p), \tag{16}$$

$$\frac{\partial P_1(x,p)}{\partial t} = \frac{1}{\hbar}\frac{\partial H_1(x,p)}{\partial x}\frac{\partial P_1(x,p)}{\partial p} - \frac{1}{\hbar}\frac{\partial H_1(x,p)}{\partial p}\frac{\partial P_1(x,p)}{\partial x} + \gamma_{0\to 1}P_0(x,p) - \gamma_{1\to 0}P_1(x,p), \tag{17}$$

where

$$\gamma_{0\to 1} = \frac{\Gamma}{\hbar} f(\Delta V), \tag{18}$$

$$\gamma_{1\to 0} = \frac{\Gamma}{\hbar}\left(1 - f(\Delta V)\right), \tag{19}$$

$$\Delta V = H_1 - H_0 = E_d + \sqrt{2}gx. \tag{20}$$

Here, Γ is the hybridization function,

$$\Gamma(\epsilon) = 2\pi \sum_k |V_k|^2 \delta(\epsilon_k - \epsilon). \tag{21}$$

In the wide band limit, Γ is a constant. f represents the Fermi function of the relevant electronic bath. Equations (16) and (17) can be solved using the SH methodology as described in Paper II.

B. The quantum master equation: The full QME vs. the secular approximation

To assess the validity of the CME, we will compute exact QME dynamics according to Eqs. (14) and (15). To do so, we assume that Γ is a constant (i.e., does not change with ϵ [Eq. (21)] or x) and we expand the reduced density matrix in a basis of harmonic oscillator eigenstates,

$$\begin{aligned}\frac{d\rho_0(i,j)}{dt} &= -\frac{i}{\hbar}(\epsilon_0(i)-\epsilon_0(j))\rho_0(i,j)\\ &\quad -\frac{\Gamma}{\hbar}\sum_{i',k} f(\epsilon_1(i')-\epsilon_0(k))F_{i\to i'}F_{k\to i'}\rho_0(k,j)\\ &\quad +\frac{\Gamma}{\hbar}\sum_{i',j'}(1-f(\epsilon_1(j')-\epsilon_0(j)))F_{i\to i'}F_{j\to j'}\rho_1(i',j'),\end{aligned} \tag{22}$$

$$\begin{aligned}\frac{d\rho_1(i',j')}{dt} &= -\frac{i}{\hbar}(\epsilon_1(i')-\epsilon_1(j'))\rho_1(i',j')\\ &\quad -\frac{\Gamma}{\hbar}\sum_{i,k'}(1-f(\epsilon_1(k')-\epsilon_0(i)))F_{i\to i'}F_{i\to k'}\rho_1(k',j')\\ &\quad +\frac{\Gamma}{\hbar}\sum_{i,j} f(\epsilon_1(j')-\epsilon_0(j))F_{i\to i'}F_{j\to j'}\rho_0(i,j),\end{aligned} \tag{23}$$

where $\epsilon_0(i)=\hbar\omega(i+\frac{1}{2})$, and $\epsilon_1(i')=\hbar\omega(i'+\frac{1}{2})+\bar{E}_d$. $\bar{E}_d$ is the renormalized impurity energy level,

$$\bar{E}_d \equiv E_d - E_r, \tag{24}$$

where $E_r \equiv g^2/\hbar\omega$ is the reorganization energy. i (i') labels a phonon mode centered at x = 0 ($x=-\sqrt{2}g/\hbar\omega$). F is the Franck-Condon factor,

$$F_{i\to i'} = \langle i'|i\rangle = \int dx\phi_{i'}(x+\sqrt{2}\lambda)\phi_i(x), \lambda \equiv g/\hbar\omega, \tag{25}$$

where $\phi_i(x)$ is the ith eigenfunction of the harmonic oscillator. The Franck-Condon factor can be expressed as[32,33]

$$F_{i\to i'} = (p!/Q!)^{1/2}\lambda^{Q-p}e^{-\lambda^2/2}L_p^{Q-p}(\lambda^2)\mathrm{sgn}(p-Q)^{p-Q}. \tag{26}$$

p (Q) is the minimum (maximum) of i and i', and L_n^m is generalized Laguerre polynomial. Equations (22) and (23) represent full, nonsecular QME dynamics which we will abbreviate "nQME." Often in the literature, when solving the QME, one makes a secular approximation–whereby one eliminates the fast oscillating off-diagonal terms of the reduced density matrix and focuses only on the diagonal matrix elements. In this case, the secular approximation of the QME (sQME) dynamical equations of motion is

$$\frac{dP_i^n}{dt} = \sum_{n',i'}[P_{i'}^{n'}W_{i'\to i}^{n'\to n} - P_i^n W_{i\to i'}^{n\to n'}], \quad n(n')=0,1, \tag{27}$$

with

$$W_{i\to i'}^{0\to 1} = \frac{\Gamma}{\hbar}|F_{i\to i'}|^2 f\left(\bar{E}_d+\hbar\omega(i'-i)\right), \tag{28}$$

$$W_{i'\to i}^{1\to 0} = \frac{\Gamma}{\hbar}|F_{i\to i'}|^2\left(1-f(\bar{E}_d+\hbar\omega(i'-i))\right), \tag{29}$$

$$W_{i\to i'}^{n\to n'} = 0, \quad n=n'. \tag{30}$$

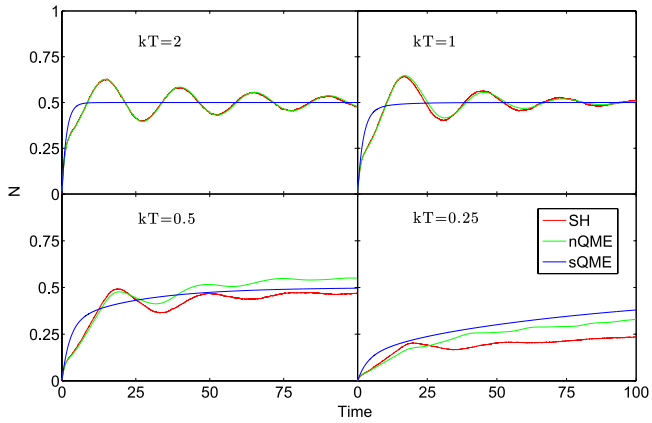

FIG. 1. Transient dynamics: the impurity electron population as a function of time. $\Gamma=1$, $\hbar\omega=0.3$, e-ph coupling $g=0.75$, $\bar{E}_d=0$. Note that SH and nQME agree at high temperatures. The sQME does not show any oscillations in electronic population, whereas the nQME shows transient oscillations which are (empirically) close to the frequency ω. At time zero, the phonon is prepared to be equilibrated thermally (assuming the impurity is unoccupied).[34]

Equations (27)-(30) were studied in Paper II. It is easy to show that, for the case of one bath, the nQME (Eqs. (22)-(26)) and the sQME (Eqs. (27)-(30)) yield the same equilibrium density matrix.

Figures 1 and 2 compare the transient dynamics for electron population according to sQME, nQME, and CME for different parameters (for all the plots here and below, we have set $\hbar=1$). We prepare the system initially with the phonon equilibrated thermally assuming that the impurity state (or level) is unoccupied (state 0). For both sQME and nQME, we use 4th order Runge-Kutta to integrate the real time dynamics, and 60 vibrational states are included to achieve converged results. For SH, we average the results over 10 000 trajectories. Clearly, without including coherence of the phonon states, sQME does not capture the oscillations of the electronic population at short times. By contrast, nQME populations do show transient oscillations and CME agrees well with nQME in the

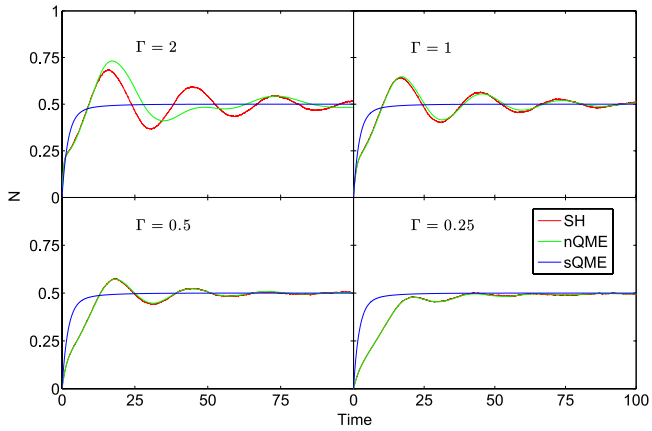

FIG. 2. Transient dynamics: the impurity electron population as a function of time. $kT=1$, $\hbar\omega=0.3$, e-ph coupling $g=0.75$, $\bar{E}_d=0$. Note that SH and nQME agree in small Γ limit. The sQME does not show any oscillations in electronic population, whereas the nQME shows transient oscillations which are (empirically) close to the frequency ω. At time zero, the phonon is prepared to be equilibrated thermally (assuming the impurity is unoccupied).[34]

limit of high temperature and small Γ. Interestingly, whereas Ref. 31 suggests that the CME can be accurate only when $\hbar\omega \ll \Gamma$, we find empirically that the CME is accurate in our simulations provided only that $\hbar\omega, \Gamma \ll kT$.

III. ELECTRON TRANSFER (ET) RATE FOR THE AH MODEL

Even though the transient populations of the impurity level exhibit oscillations at short times, after reaching equilibrium, one finds equal and opposite fluxes in population from one diabat to the other. These fluxes will now be shown to be those derived from the corresponding Marcus rates.

A. Standard electron transfer: Marcus theory for the spin-boson model

For a spin-boson model with two electronic states D and A that correspond to the system states before and after an ET step, the ET rate is given by the Marcus rate

$$k_{D\to A} = \frac{2\pi}{\hbar}|V_{DA}|^2\mathcal{F}(E_{AD}). \tag{31}$$

Here, $E_{AD} \equiv E_A - E_D$ is the difference in energy between relaxed donor and acceptor (i.e., the "driving force") and $\mathcal{F}$ is the density weighted Frank-Condon factor which, in the classical limit, takes the form

$$\mathcal{F}(E_{AD}) = \frac{e^{-(E_r+E_{AD})^2/4E_rkT}}{\sqrt{4\pi E_r kT}}. \tag{32}$$

E_r is the reorganization energy. In the corresponding electrode process, taking the process $D \to A$ to imply an electron given from the impurity to the metal, the initial and final states are replaced by manifolds of system-metal states and the rate is obtained by averaging over the thermal distribution of initial states and summing over all final states. This leads to[35]

$$k_{D\to A} = \int d\epsilon\Gamma(\epsilon)(1-f(\epsilon))\mathcal{F}(E_{AD}+\epsilon), \tag{33}$$

$$k_{A\to D} = \int d\epsilon\Gamma(\epsilon)f(\epsilon)\mathcal{F}(E_{DA}-\epsilon), \tag{34}$$

where $\Gamma(\epsilon) = 2\pi\sum_k |V_k|^2\delta(\epsilon_k - \epsilon)$ is the hybridization function defined in Eq. (21), taken below to be energy independent. Finally note that in the AH model, $E_{DA} = -E_{AD} = \bar{E}_d$ is the renormalized single electron energy defined by Eq. (24).

B. Agreement with the SH picture

Let us now show that the CME yields the same Marcus rate in the long time (equilibrium) limit.[36]

In Paper II, we have shown that at equilibrium, the probability densities $P_1(x,p)$ and $P_0(x,p)$ reach a Boltzmann distribution. Thus, the normalized reduced probability densities for position will be

$$P_1(x) = \sqrt{\frac{\hbar\omega}{2\pi kT}}e^{-\frac{1}{2}\hbar\omega(x+\sqrt{2}g/\hbar\omega)^2/kT}, \tag{35}$$

$$P_0(x) = \sqrt{\frac{\hbar\omega}{2\pi kT}}e^{-\frac{1}{2}\hbar\omega x^2/kT}. \tag{36}$$

From the CME (Eqs. (16)-(20)), the ET rate from state 1 to state 0 (representing an electron hopping from the impurity to the bath) at position x is determined as $\Gamma(1 - f(\sqrt{2}gx + E_d))$. On average, the rate is

$$k_{1\to 0} = \int dx\Gamma(1-f(\sqrt{2}gx+E_d)) \times\sqrt{\frac{\hbar\omega}{2\pi kT}}e^{-\frac{1}{2}\hbar\omega(x+\sqrt{2}g/\hbar\omega)^2/kT}. \tag{37}$$

Now, if we define $\sqrt{2}gx + E_d \equiv \epsilon$ and change variables from x to ϵ (using $E_r = g^2/\hbar\omega$ and $\bar{E}_d = E_d - E_r$), the above equation becomes

$$k_{1\to 0} = \int d\epsilon\Gamma(1-f(\epsilon))\frac{e^{-(E_r+\epsilon-\bar{E}_d)^2/4E_rkT}}{\sqrt{4\pi E_r kT}}, \tag{38}$$

which agrees with Eq. (33). Similarly, one can show the backward rate from SH is given by

$$k_{0\to 1} = \int dx\Gamma f(\sqrt{2}gx+E_d)P_0(x). \tag{39}$$

Equation (39) can be rewritten to recover the standard ET result (Eq. (34)),

$$k_{0\to 1} = \int d\epsilon\Gamma f(\epsilon)\frac{e^{-(E_r-\epsilon+\bar{E}_d)^2/4E_rkT}}{\sqrt{4\pi E_r kT}}. \tag{40}$$

This proves the equivalence we hypothesized.

Moreover, in the SH picture, these ET rates can be easily extended to the case where Γ is not a constant, but depends on the nuclear position x. Below, we consider the case where $\Gamma = \Gamma_0\exp(-Dx^2)$. This is equivalent to replacing d^+ (d) with $d^+e^{-Dx^2/2}$ ($de^{-Dx^2/2}$) in system-bath coupling Hamiltonian (Eq. (4)).

IV. BROADENING BY THE MARCUS RATE

From Eqs. (37)-(40), one can show that the forward and backward Marcus rates satisfy detailed balance,

$$k_{1\to 0} = e^{\bar{E}_d/kT}k_{0\to 1}, \tag{41}$$

where $\bar{E}_d$ is defined in Eq. (24). Equation (41) proves that the equilibrium impurity electron population is a Fermi function,

$$N = \frac{k_{0\to 1}}{k_{0\to 1}+k_{1\to 0}} = \frac{1}{1+e^{\bar{E}_d/kT}} = f(\bar{E}_d), \tag{42}$$

which follows from detailed balance (Eq. (41)).

It is important to remember that Eq. (42) is correct only in the limit of vanishingly small Γ. This expression does not include any broadening of the impurity level. To incorporate such broadening, in Paper II, we broadened all electronic observables using a Lorentzian function of width Γ. This worked well in certain regimes. However, this ansatz is not general and it is not clear how to define a broadening width if Γ is not a constant, but rather depends on nuclear coordinates. For instance, $\Gamma(x) = \Gamma_0 e^{-Dx^2}$.

Numerical tests described below indicate that a convolution of all electronic observables with a Lorentzian whose width is given by the sum of forward and backward Marcus

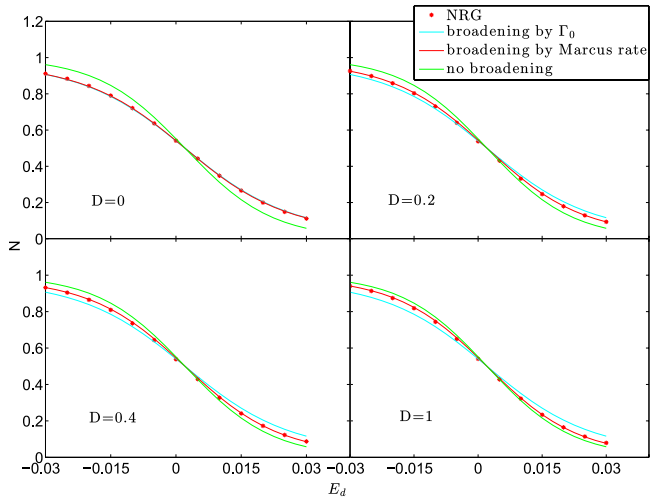

FIG. 3. The equilibrium electron population as a function of the impurity energy level, when Γ depends on nuclear coordinate, $\Gamma = \Gamma_0 e^{-Dx^2}$, $\Gamma_0 = 0.01$, $kT = 0.01$, $\hbar\omega = 0.003$, e-ph coupling $g = 0.0025$. The Marcus rates appear to be good estimates for a broadening rate. NRG data can be considered nearly exact.[4,37]

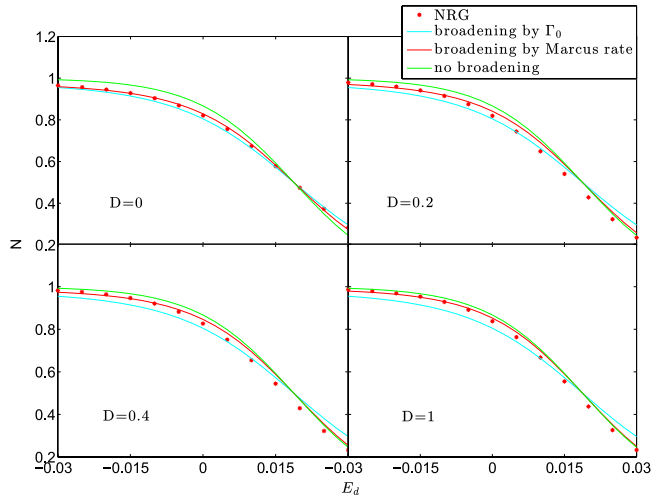

FIG. 4. The equilibrium electron population as a function of the impurity energy level, when Γ depends on nuclear coordinate, $\Gamma = \Gamma_0 e^{-Dx^2}$, $\Gamma_0 = 0.01$, $kT = 0.01$, $\hbar\omega = 0.003$, e-ph coupling $g = 0.0075$. The Marcus rates appear to be good estimates for a broadening rate. NRG data can be considered nearly exact.[4,37]

rates,

$$\gamma_t = k_{0\to1} + k_{1\to0}, \tag{43}$$

provides a good approximation as compared with numerically exact NRG results. This observation is intuitively appealing, since Eq. (43) is the inverse lifetime of an electron (hole) in an occupied (unoccupied) molecular level. Applying such broadening to Eq. (42), the impurity level occupation takes the form

$$N = \int dE \frac{1}{2\pi} \frac{\gamma_t}{(\gamma_t/2)^2 + (E - \bar{E}_d)^2} f(E), \tag{44}$$

that can be compared to the NRG-calculated value. As shown in Figures 3 and 4, the results from Eq. (44) agree well with NRG. For comparison, we also plot results either (i) without broadening or (ii) after broadening by Γ_0,

$$N = \int dE \frac{1}{2\pi} \frac{\Gamma_0}{(\Gamma_0/2)^2 + (E - \bar{E}_d)^2} f(E). \tag{45}$$

Note when $D = 0$, $\Gamma = \Gamma_0$.

To highlight some of the nuances we face in estimating broadening rates, in Figures 5(a) and 5(b), we plot the electron population as a function of (a) e-ph coupling g and (b) temperature T. In Figure 5(a), we find that, even though results from Marcus rate broadening are not perfect (as compared to the NRG results), Marcus rate broadening clearly captures the feature that increasing g reduces the effective broadening. In Figure 5(b), we note that Marcus rate broadening agrees with NRG for both high and low temperatures.

Overall, Eq. (44) is the best approximation among all broadening approaches we have tested thus far. Future work will likely explore further the data in Figures 3-5 and seek either a better approach or an improved theoretical foundation for this empirical broadening behavior.

V. STEADY STATE CURRENT

Thus far, we have shown that when impurity-bath coupling depends strongly on nuclear coordinates, SH shows good

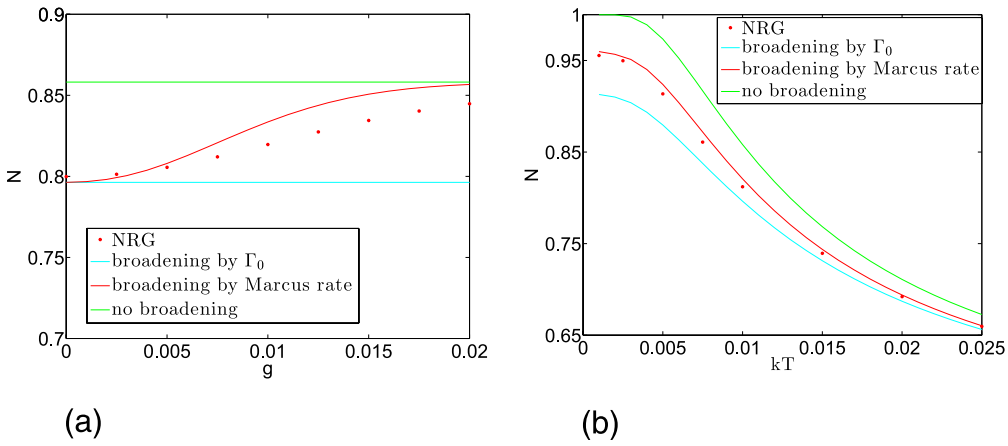

FIG. 5. The equilibrium electron population as a function of (a) e-ph coupling g and (b) temperature kT. The other parameters are $D = 0$, $\Gamma_0 = 0.01$, $\hbar\omega = 0.003$, $\bar{E}_d = -0.018$. Note that broadening by the Marcus rate gives the qualitatively correct behavior. NRG data can be considered nearly exact.[4,37] (a) $kT = 0.01$. (b) $g = 0.0075$.

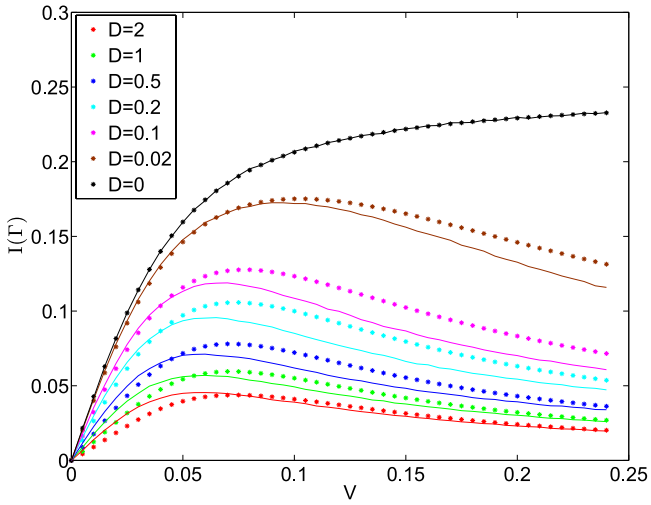

FIG. 6. I-V curves for different values of D (see Eq. (46)). Lines from SH, dots from the sQME. $g = 0.005$, $\hbar\omega = 0.003$, $kT = 0.01$, $\Gamma = 2\Gamma_0 = 0.01$, $\bar{E_d} = 0$. For large D, we observe negative differential resistance.

agreement with NRG for equilibrium quantities (i.e., population). With this in mind, we will now study out of equilibrium quantities; in particular, we will compare I-V curves from SH and sQME in case of two electronic baths.[7,38,39] Our interest is exploring the rich nonequilibrium physics possible when Γ strongly depends on x, which might be called "non-Condon" behavior. Our choice here of hybridization is

$$\Gamma_L = \Gamma_0 e^{-Dx^2}, \tag{46}$$

$$\Gamma_R = \Gamma_0. \tag{47}$$

The procedure for calculating I-V curves for SH and QME can be found in Paper II. In short, with two electronic baths (with Fermi levels μ_L and μ_R), the hopping rates of the CME (compared with the case of one electronic bath [Eqs. (18) and (19)]) will be

$$\gamma_{0\to1} = \frac{\Gamma_L}{\hbar} f^L(\Delta V) + \frac{\Gamma_R}{\hbar} f^R(\Delta V), \tag{48}$$

$$\gamma_{1\to0} = \frac{\Gamma_L}{\hbar}(1 - f^L(\Delta V)) + \frac{\Gamma_R}{\hbar}(1 - f^R(\Delta V)). \tag{49}$$

Γ_L (Γ_R) is the hybridization function of the impurity coupled to the left (right) electronic bath. The CME (Eqs. (16) and (17)) will be unchanged. The current can be calculated using the steady states probability densities $P_0(x,p)$ and $P_1(x,p)$,

$$I = \int dxdp\Big(\gamma^L_{0\to1}(x)P_0(x,p) - \gamma^L_{1\to0}(x)P_1(x,p)\Big), \tag{50}$$

with

$$\gamma^L_{0\to1} = \frac{\Gamma_L}{\hbar} f^L(\Delta V), \tag{51}$$

$$\gamma^L_{1\to0} = \frac{\Gamma_L}{\hbar}(1 - f^L(\Delta V)). \tag{52}$$

For the sQME, when $\Gamma_L = \Gamma_0 e^{-Dx^2}$, it is easy to show that the transition rates between the impurity and the left electrode become (compared to Eqs. (28)-(30))

$$W^{0\to1^L}_{i\to i'} = \frac{\Gamma_0}{\hbar}|\langle i|e^{-Dx^2/2}|i'\rangle|^2 f^L\Big(\bar{E_d} + \hbar\omega(i' - i)\Big), \tag{53}$$

$$W^{1\to0^L}_{i'\to i} = \frac{\Gamma_0}{\hbar}|\langle i|e^{-Dx^2/2}|i'\rangle|^2\Big(1 - f^L(\bar{E_d} + \hbar\omega(i' - i))\Big), \tag{54}$$

$$W^{n\to n'^L}_{i\to i'} = 0, \quad n = n', \tag{55}$$

where again i (i') labels a phonon mode centered at x = 0 ($x = -\sqrt{2}g/\hbar\omega$). The transition rates between the impurity and the right electrode are unchanged; one just sets $f = f^R$ in Eqs. (28)-(30). As implemented in the sQME, the final on and off rates are the sum of the left and right rates,

$$W^{n'\to n}_{i'\to i} = W^{n'\to n^L}_{i'\to i} + W^{n'\to n^R}_{i'\to i}. \tag{56}$$

Similar to Eq. (50), with the steady states probability densities P^n_i, we can calculate the steady current

$$I = \sum_{ii'} P^0_i W^{0\to1^L}_{i\to i'} - P^1_{i'} W^{1\to0^L}_{i'\to i}. \tag{57}$$

To obtain converged results for the current, 300 phonon states are kept for the sQME. Here, we do not incorporate any level broadening for either the sQME or SH data (which is valid when Γ is small).

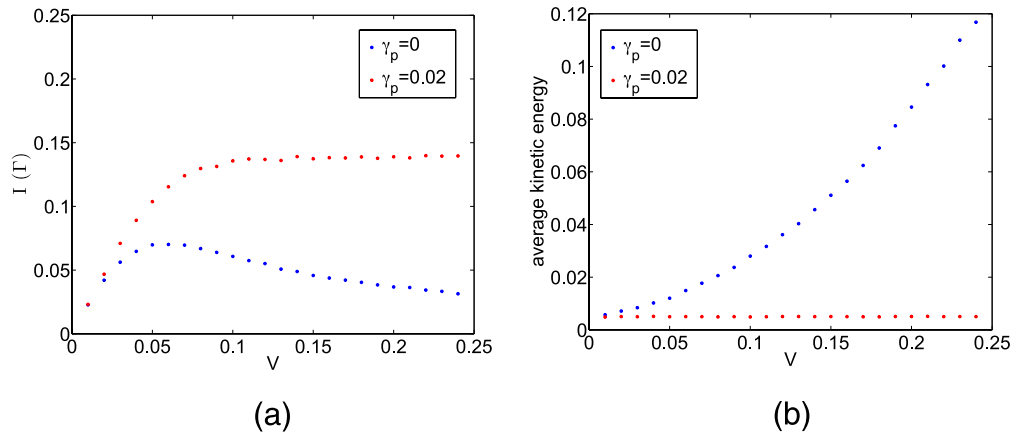

FIG. 7. (a) I-V curves with and without an extra phonon bath, (b) the average kinetic energy (effective temperature) of the oscillator as a function of bias. $kT = 0.01$, $\Gamma_0 = 0.01$, $D = 0.5$, $\hbar\omega = 0.003$, $\bar{E_d} = 0$, e-ph coupling $g = 0.0075$, the damping term $\gamma_P = 0.02$. For weak phonon damping, negative differential resistance goes hand in hand with a voltage-dependent heating. For strong phonon damping, however, the average kinetic energy is independent of voltage and we find no negative differential resistance.

In Figure 6, we plot I-V curves for different values of D from SH and sQME, and we find good agreement between them.

The most interesting observation in Figure 6 is that, when D is nonzero, the I-V curve shows a peak. In words, increasing the voltage across the impurity can lower the current. This peak can be explained by the (unbroadened) Landauer formula,

$$I = \frac{\Gamma_L \Gamma_R}{\Gamma_L + \Gamma_R}(f^L - f^R). \tag{58}$$

In the normal region, when the bias between the two Fermi levels becomes larger ($f^L - f^R$ becomes larger), current increases. However, in addition to this primary effect, increasing the bias will also heat the oscillator to a higher temperature than the bath.[33,40,41] Thus, on average, the root of mean square displacement $\langle x^2 \rangle$ should increase, which reduces the average of Γ_L, due to the factor e^{-Dx^2}. From the Landauer formula, when Γ_L becomes smaller, the current decreases.

As evidence for this explanation, in our SH calculations, we have added an external phonon bath coupled to the oscillator both through a Langevin force and a damping term.[42] Figure 7(b) shows that if the damping term γ_p is set to be $\gamma_p = 0.02$, the temperature of the oscillator will not change with the voltage. In this case, observe that there are now no peaks in the I-V curves (Figure 7(a)). By contrast, without friction, the temperature of the oscillator changes dramatically with bias, and the I-V curves do show a peak.

VI. CONCLUSION

We have investigated the transient dynamics of the CME, which include interesting oscillations at short times. For large enough temperature T, our dynamics agree with the full, non-secular QME at most times. The secular QME provides a good approximation to the full QME at steady states.

To connect with standard nonadiabatic quantum dynamics, we have shown analytically that our SH approach recovers the celebrated Marcus rate when Γ is a constant. Moreover, SH can be extended easily to the case where the hybridization function depends on the nuclear coordinate. In such a case, the Marcus rate gives us an easy, approximate way to incorporate level broadening, which has been verified by comparing with NRG for equilibrium populations (and with secular QME for out of equilibrium I-V curves). If possible, further benchmarking against exact dynamics will be useful. For now, we believe it is promising to apply the CME to a real condensed phase system—for example, the interaction between an adsorbate and a metal surface, which depends strongly on position. This work is ongoing.

Finally, we have studied I-V curves for the case where $\Gamma = \Gamma_0 e^{-Dx^2}$, and we have found an interesting turnover effect. This turnover can be explained as the result of heating from a steady state current and offers yet another example of inelastic scattering (which can lead to instability,[33,40] and I-V step feathers[10,30]). With coupling to an external phonon bath, however, the turnover effect disappears.

Overall, given the fact that Γ will hardly ever be a constant in practice, we believe the paper represents an important step forward towards understanding SH and implementing an algorithm to simulate a realistic condensed phase system.

ACKNOWLEDGMENTS

We thank Guy Cohen for very useful conversations. This material is based upon work supported by the U.S. Air Force Office of Scientific Research (USAFOSR) PECASE award under AFOSR Grant No. FA9950-13-1-0157. J.E.S. acknowledges a Cottrell Research Scholar Fellowship and a David and Lucille Packard Fellowship.

[1]T. Holstein, Ann. Phys. **8**, 325 (1959).
[2]G. Cohen, E. Gull, D. R. Reichman, and A. J. Millis, Phys. Rev. Lett. **112**, 146802 (2014).
[3]A. C. Hewson and D. Meyer, J. Phys.: Condens. Matter **14**, 427 (2002).
[4]R. Bulla, T. A. Costi, and T. Pruschke, Rev. Mod. Phys. **80**, 395 (2008).
[5]K. G. Wilson, Rev. Mod. Phys. **47**, 773 (1975).
[6]M. Thoss, I. Kondov, and H. Wang, Phys. Rev. B **76**, 153313 (2007).
[7]L. Mühlbacher and E. Rabani, Phys. Rev. Lett. **100**, 176403 (2008).
[8]M. Brandbyge, P. Hedegård, T. F. Heinz, J. A. Misewich, and D. M. Newns, Phys. Rev. B **52**, 6042 (1995).
[9]N. Bode, S. V. Kusminskiy, R. Egger, and F. von Oppen, Beilstein J. Nanotechnol. **3**, 144 (2012).
[10]M. Galperin, M. A. Ratner, and A. Nitzan, J. Phys.: Condens. Matter **19**, 103201 (2007).
[11]W. Ding, C. F. A. Negre, L. Vogt, and V. S. Batista, J. Phys. Chem. C **118**, 8316 (2014).
[12]V. Mujica, M. Kemp, and M. A. Ratner, J. Chem. Phys. **101**, 6849 (1994).
[13]J. R. Reimers, G. C. Solomon, A. B. A. Gagliardi, N. S. Hush, T. Frauenheim, A. D. Carlo, and A. Pecchia, J. Phys. Chem. A **111**, 5692 (2007).
[14]J. C. Tully, J. Chem. Phys. **93**, 1061 (1990).
[15]J. C. Tully and R. K. Preston, J. Chem. Phys. **55**, 562 (1971).
[16]W. Ouyang, W. Dou, and J. E. Subotnik, J. Chem. Phys. **142**, 084109 (2015).
[17]R. K. Preston and J. S. Cohen, J. Chem. Phys. **65**, 1589 (1976).
[18]N. Shenvi, S. Roy, and J. C. Tully, J. Chem. Phys. **130**, 174107 (2009).
[19]N. Shenvi, S. Roy, and J. C. Tully, Science **326**, 829 (2009).
[20]N. Shenvi, J. R. Schmidt, S. T. Edwards, and J. C. Tully, Phys. Rev. A **78**, 022502 (2008).
[21]L. Chen, T. Hansen, and I. Franco, J. Phys. Chem. C **118**, 20009 (2014).
[22]J. E. Subotnik, T. Hansen, M. A. Ratner, and A. Nitzan, J. Chem. Phys. **130**, 144105 (2009).
[23]T. Zelovich, L. Kronik, and O. Hod, J. Chem. Theory Comput. **10**, 2927 (2014).
[24]S. Ajisaka, F. Barra, C. Mejía-Monasterio, and T. Prosen, Phys. Scr. **86**, 058501 (2012).
[25]C. G. Sánchez, M. Stamenova, S. Sanvito, D. R. Bowler, A. P. Horsfield, and T. N. Todorov, J. Chem. Phys. **124**, 214708 (2006).
[26]E. J. McEniry, D. R. Bowler, D. Dundas, A. P. Horsfield, C. G. Sánchez, and T. N. Todorov, J. Phys.: Condens. Matter **19**, 196201 (2007).
[27]W. Dou, A. Nitzan, and J. E. Subotnik, J. Chem. Phys. **142**, 084110 (2015).
[28]M. A. Gata and P. R. Antoniewicz, Phys. Rev. B **47**, 13797 (1993).
[29]Y. Huang, C. T. Rettner, D. J. Auerbach, and A. M. Wodtke, Science **290**, 111 (2000).
[30]M. Galperin, M. A. Ratner, and A. Nitzan, Nano Lett. **5**, 125 (2005).
[31]F. Elste, G. Weick, C. Timm, and F. V. Oppen, Appl. Phys. A **93**, 345 (2008).
[32]J. Koch, F. von Oppen, Y. Oreg, and E. Sela, Phys. Rev. B **70**, 195107 (2004).
[33]J. Koch, M. Semmelhack, F. von Oppen, and A. Nitzan, Phys. Rev. B **73**, 155306 (2006).
[34]For the QME, the original statistics are quantum, whereas for the CME we choose initial conditions according to classical statistics (rather than the Wigner distribution).
[35]A. Nitzan, *Chemical Dynamics in Condensed Phase* (Oxford University Press, 2006).
[36]To understand why CME rates should agree with Marcus rates at equilibrium, we observe that Marcus theory is a transition state theory

(TST) for the electron transfer rate, that relies on the two standard TST assumptions: (a) the reactant state is in thermal equilibrium and (b) back-scattering processes may be disregarded in the rate calculation. The second assumption is already implemented in the second order rates that enter the master equation (16)–(19).

[37]For NRG calculations, the band width is $W = 1$, the basis is initialized with 100 boson states, the maximum number of eigenstates kept is $N_s = 1500$, and the logarithmic discretizing parameter is $\Lambda = 2$.

[38]G. Cohen, E. Gull, D. R. Reichman, A. J. Millis, and E. Rabani, Phys. Rev. B **87**, 195108 (2013).

[39]In the future, we intend to benchmark some time dependent calculation against exact results from path integral Monte Carlo.[7,38]

[40]K. Kaasbjerg, T. Novotný, and A. Nitzan, Phys. Rev. B **88**, 201405 (2013).

[41]L. Siddiqui, A. W. Ghosh, and S. Datta, Phys. Rev. B **76**, 085433 (2007).

[42]B. R. Landry and J. E. Subotnik, J. Chem. Phys. **137**, 22A513 (2012).